PIT Project

Behaviour of steel framed structures under fire conditions

British Steel Fire Test3:
Reference ABAQUS model using grillage representation for slab

Research Report

Report R00-MD10

Abdel Moniem Sanad

The University of Edinburgh
School of Civil & Environmental Engineering
Edinburgh, UK

June, 2000

TABLE OF CONTENTS

LIST OF FIGURES :

NOTES:

1. In the description of the numerical model below we use the following terms :
2. “the plane” to define the plane of the floor.
3. “joist” means a steel beam, and the “test joist” means the heated joist during the fire test.
4. “vertical” means vertical to the slab plane.
5. “in-plane” means in the plane of the slab.
6. “joist longitudinal direction” or “longitudinal direction” to mean parallel to the joist length coordinate.
7. “transverse direction” to mean at right angle to the joist longitudinal direction (i.e. in the direction of the longitudinal axis of the ribs).
8. “Reference vertical coordinate” is the interface between the slab and joist.

1. GEOMETRIC DESCRIPTION

1.1. Layout

The test was performed on the second floor of the building to study the behaviour of a complete floor system and in particular the membrane action. The compartment of approximately 80m^2 was built on the first floor in one corner of the structure. To achieve the required level of thermal loading (around 1000°C), a real fire was created, with a fire loading of 45 kg of wood/m^2 and the ventilation was provided by a an adjustable 7m wide opening. The tested floor contains 4 unprotected beams and 2 protected edge beams. All secondary beams are equally spaced and have 9m span connected semi-rigidly to columns or to primary beams. The heated primary beam has a length of 6m. All columns were protected along their full height. The composite profiled deck slab has a span of 3m between secondary beams. Figure 1 shows the layout of the test and the location of the deflections measurements.

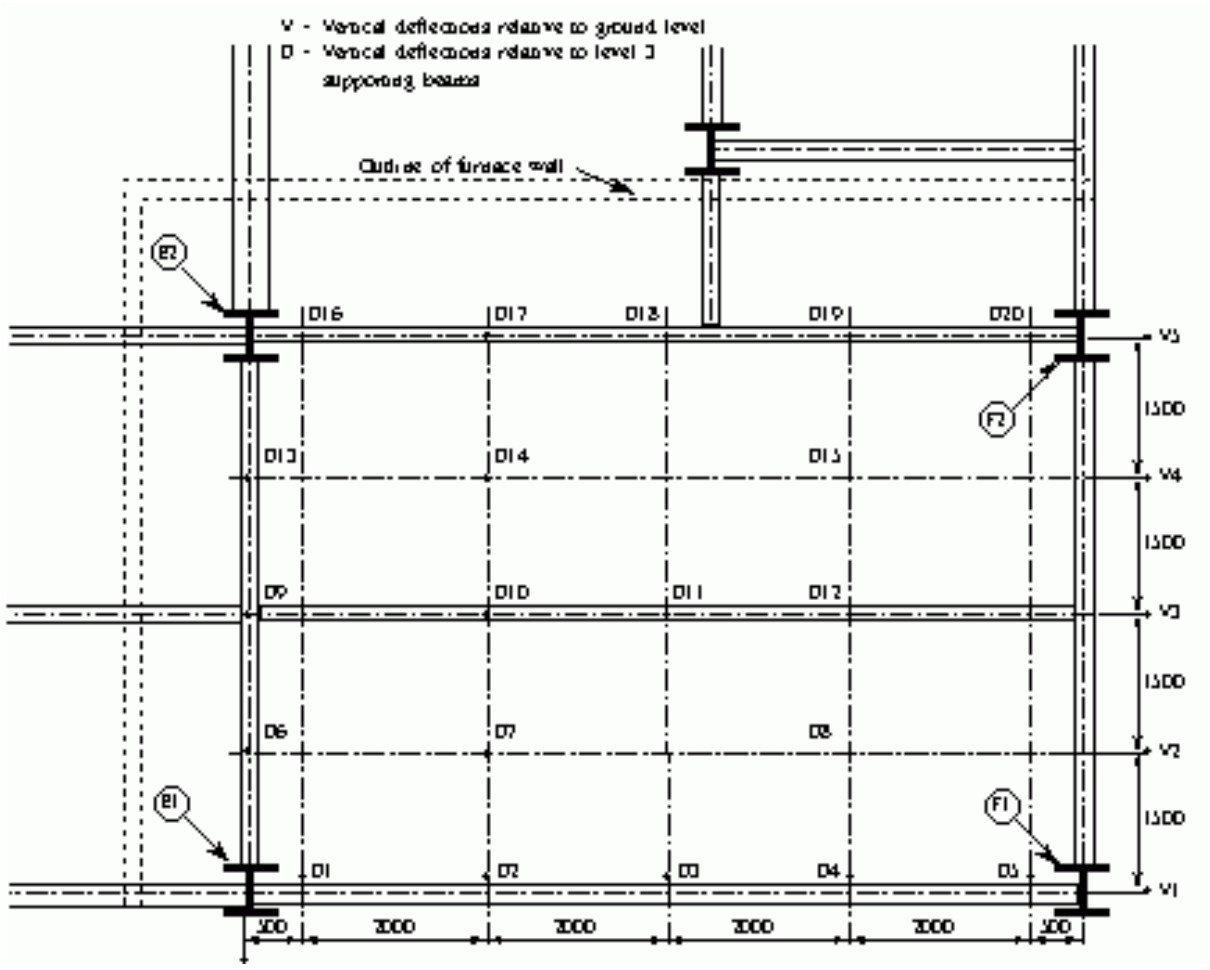

Layout of Test3
Figure 1

1.2. Finite element mesh

Figure 2 shows the finite element model of the test. The area affected by the fire is indicated by dashed lines. In the direction of the secondary beams (longitudinal), the model starts from the corner of the structure, covers the heated compartment and extends to the end of the span beyond the compartment to include the membrane forces expected to develop during the fire. In the transverse direction (direction parallel to the slab ribs), the model starts from the edge of the building, cover the heated compartment and extends to the centreline of the building for the same reason. In the model, each structural steel member is idealised by an appropriate beam element.

Figure 3 shows the typical cross-section of the steel members, Table 1 gives the dimensions of the primary and secondary joists respectively. The centroid of the secondary joists is located 152.5mm below the reference vertical co-ordinate of the joist's top flange. The centroid of the primary and edge joists is located 178mm below the reference level. The column is modelled using a similar beam elements.

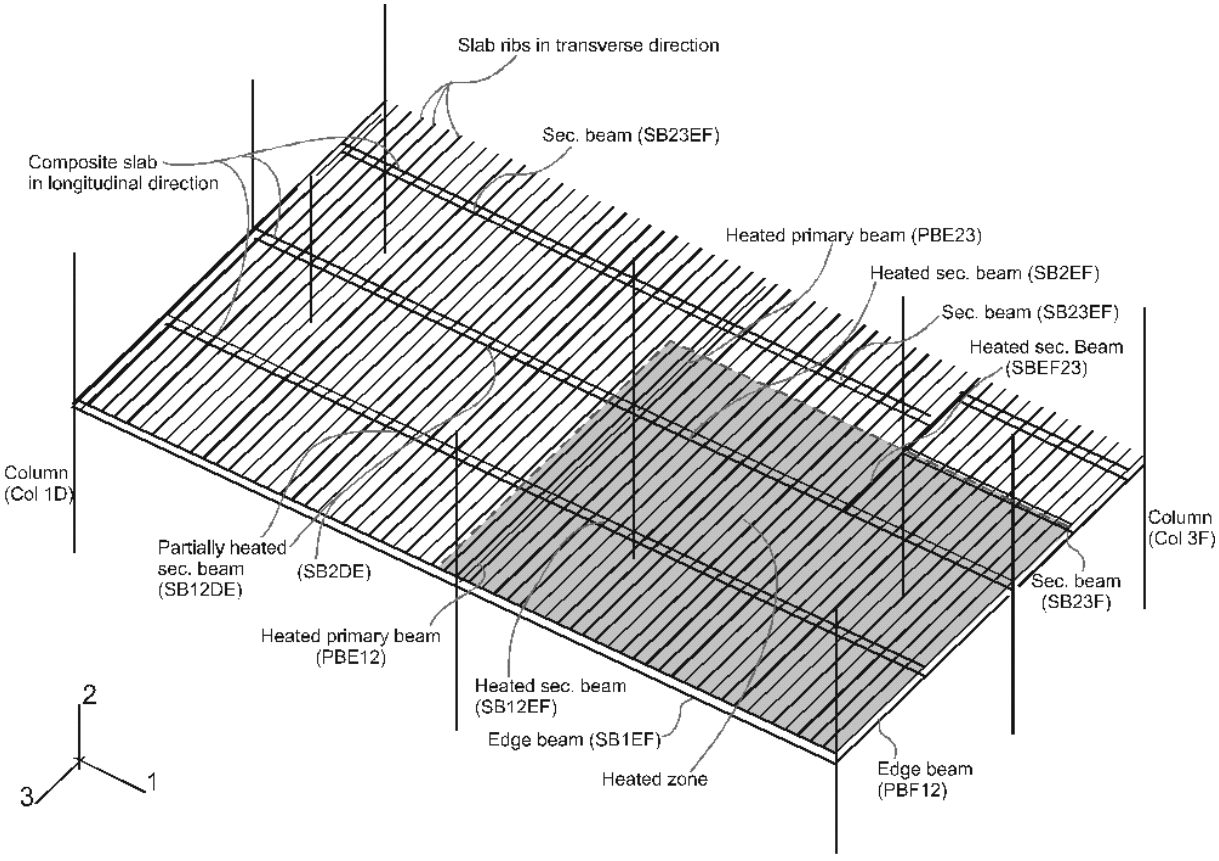

Model of fire test3

Figure 2

The slab behaviour is modelled by a grillage type idealisation using beam elements to represent the slab behaviour in both the longitudinal and transverse directions. In the longitudinal direction (X), the slab element has a rectangular section with 70mm depth and an effective width equal to 2250mm, calculated according to the Eurocode 4 (ENV1994) for a simply supported beam case. In

the transverse direction (Y), slab elements have a trapezoidal shape and the geometry of the concrete section in this direction is shown in Figure 4. The thickness of the steel deck used is 9mm. Reinforcement of one layer of A142 mesh was provided. Table 2 gives the dimensions of the sections in both directions.

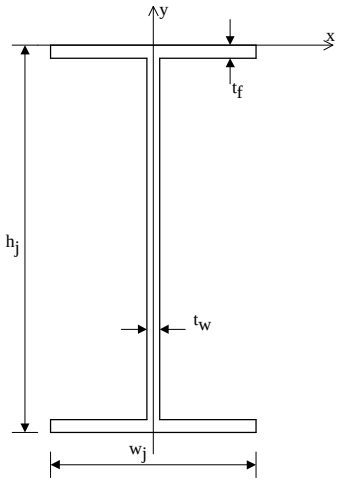

Typical cross section of the steel beams

Figure 3

	h_j (mm)	w_j (mm)	t_f (mm)	t_w (mm)
Primary & Edge beams (H)	**355.6**	**171.5**	**11.5**	**7.3**
Secondary beams (L)	**303.8**	**151.9**	**10.2**	**6.1**

Table 1

Dimensions of the steel members

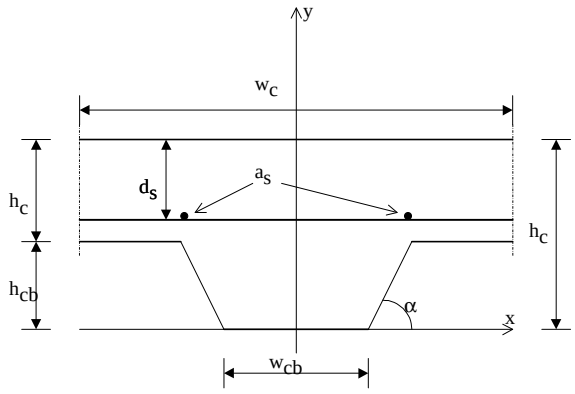

Cross section of the composite slab

Figure 4

	W_c	W_{cb}	h_{ct}	h_{cb}	α (°)	a_s	d_s
Slab in transverse direction	**300**	**136**	**70**	**60**	**65**	**42.6**	**55**
Slab in longitudinal direction	**2250**	**-**	**70**	**-**	**-**	**319.5**	**55**

Table 2

Dimensions of slab sections

2. MATERIAL BEHAVIOUR

For steel structures under high temperature the relationship between stress and strain changes considerably. At increased temperature, the material properties degrade and its capacity to deform increases which is measured by the reduction of the Young's modulus. In the finite element model, the relation between the stress and the strain under high temperature is defined according to the Eurocode 3 (ENV1993). The relation is elastic-perfect plastic at ambient temperature, and the reduction of the material properties starts at a temperature higher than 100C as shown in Figure 5. Identical material behaviour is assumed for both tension and compression.

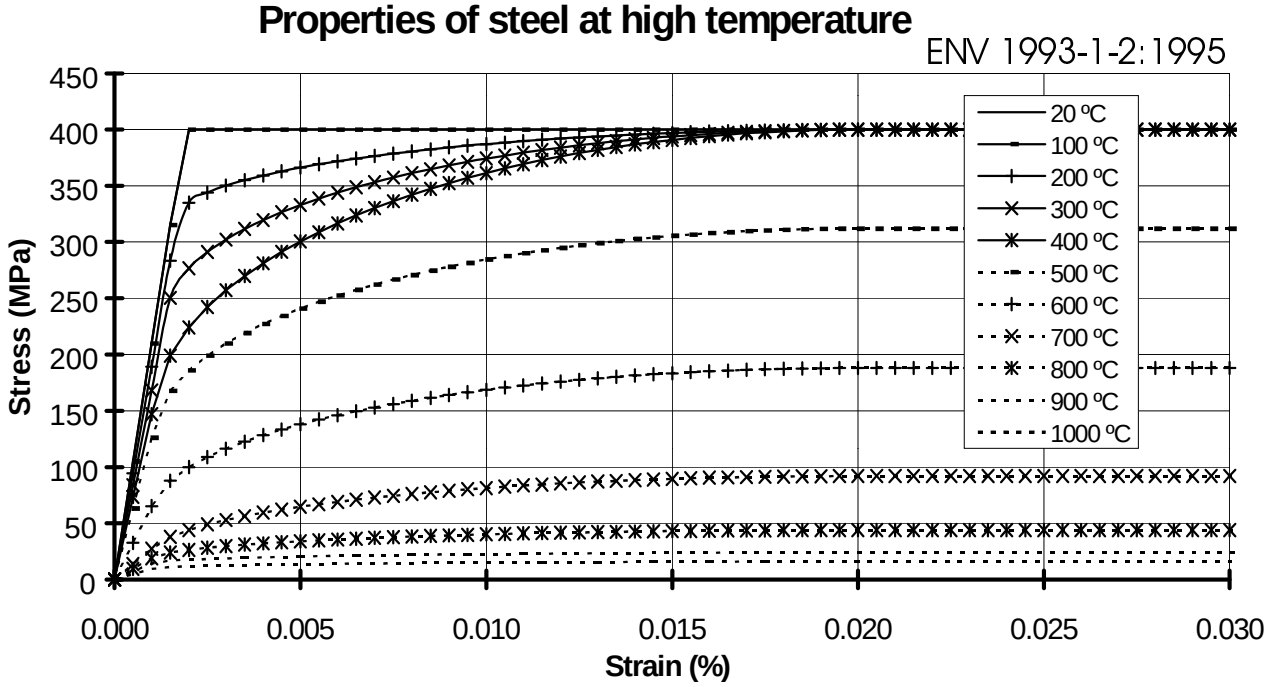

Figure 5

Steel stress-strain relationship at high temperature

Similarly, the behaviour of concrete is characterised by material property degradation with increased temperature. The stress-strain relationship is then defined according to the Eurocode 2 (ENV1992) as shown in Figure 6. Here, the initial elastic behaviour is followed by a plastic-hardening curve up to the ultimate stress, after which, a decaying zone represents the post-crushing behaviour for concrete. This relationship has the advantage of allowing the definition of a stress level for large plastic deformations, usually reached during fire conditions. It may be noted that no tension is considered in the model for the concrete at both ambient and elevated temperature, however the tensile resistance of the reinforcement and the steel deck is considered.

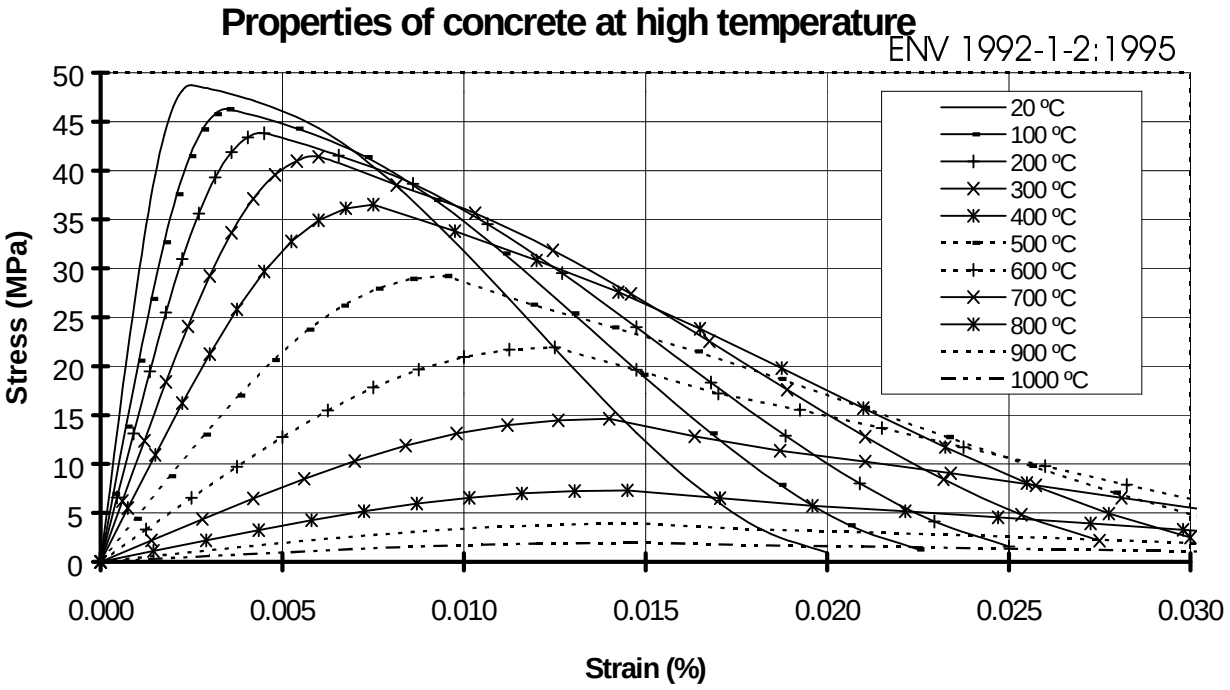

Figure 6

Concrete stress-strain relationship at high temperature

2.1. Section behaviour for steel members

For all steel members, the classic linear beam element applying the hypotheses of *plane surface remains plane* is used. Each point on the cross section, along each member, follows the stress-strain relationship (Figure 5) as a function of the point's temperature. This takes into consideration the variable temperature profile applied across the section and the corresponding material properties during different stages of the fire. The connections between different steel members (beam to column connection and beam to beam connection) are modelled by pin connections where boundary conditions are imposed on the relative displacement of the joining elements.

2.2. Slab modelling

In a reinforced concrete slab, more complex behaviour has to be modelled. The different behaviour of concrete in tension and compression, the orthotropic behaviour of concrete due to the reinforcing mesh and the decking steel and the development of membrane action need to be considered in order to provide a realistic representation of the slab behaviour. In the numerical model developed in this paper, the concrete modelling is based on the global behaviour of the concrete section, with the above factors taking into consideration. The slab is modelled by two sets of beam elements running parallel and perpendicular to the secondary beams. In each direction, the beam elements have a pre-defined force-strain and moment-curvature relationship. These relationships are calculated based on the geometry and the material properties of the section in each direction and taking into account the variable temperature over the same section and the corresponding material properties (O'Connor and al. 1995).

The behaviour of the slab in the longitudinal direction (direction of the secondary joists axis) is modelled by beam elements, using bilinear moment/curvature and force/strain relationships which are uncoupled (Figure 7,8). The yield points for the force relationship in each sense are given by the section's plastic resistance for normal force (with different values for tension and compression). The yield points for the bending relationship are given by the section's plastic resistance for bending (with different values for sagging and hogging). The post-yield behaviour is modelled by a linear relationship (moment/curvature and force/strain), decreasing from the yield point to the ultimate section resistance based on the steel reaching the limiting strain for yield strength.

The behaviour of the slab in the direction of the primary joist axis (transverse) is modelled by beam elements. The transverse bending and transverse membrane action of the slab is modelled by beam elements with their longitudinal axis in the transverse direction, using bilinear moment/curvature and force/strain relationships which are uncoupled (Figure 9,10). The yield points for the force relationship in each sense are given by the section's plastic resistance for normal force (with different values for tension and compression). The yield points for the bending relationship are given by the section's plastic resistance for bending (with different values for sagging and hogging). These beam ribs have a very high bending stiffness about the vertical axis (i.e. relating to bending deformations in the horizontal plane) this is modelled by a increasing this bending stiffness to 100 times the bending stiffness of an individual rib. Also to overcome convergence problems in the numerical solutions, the slab tension and hogging moment included hardening beyond the first yield point. The beam used in modelling the slab are 3D beam element which has linear elastic behaviour for the torsional

.

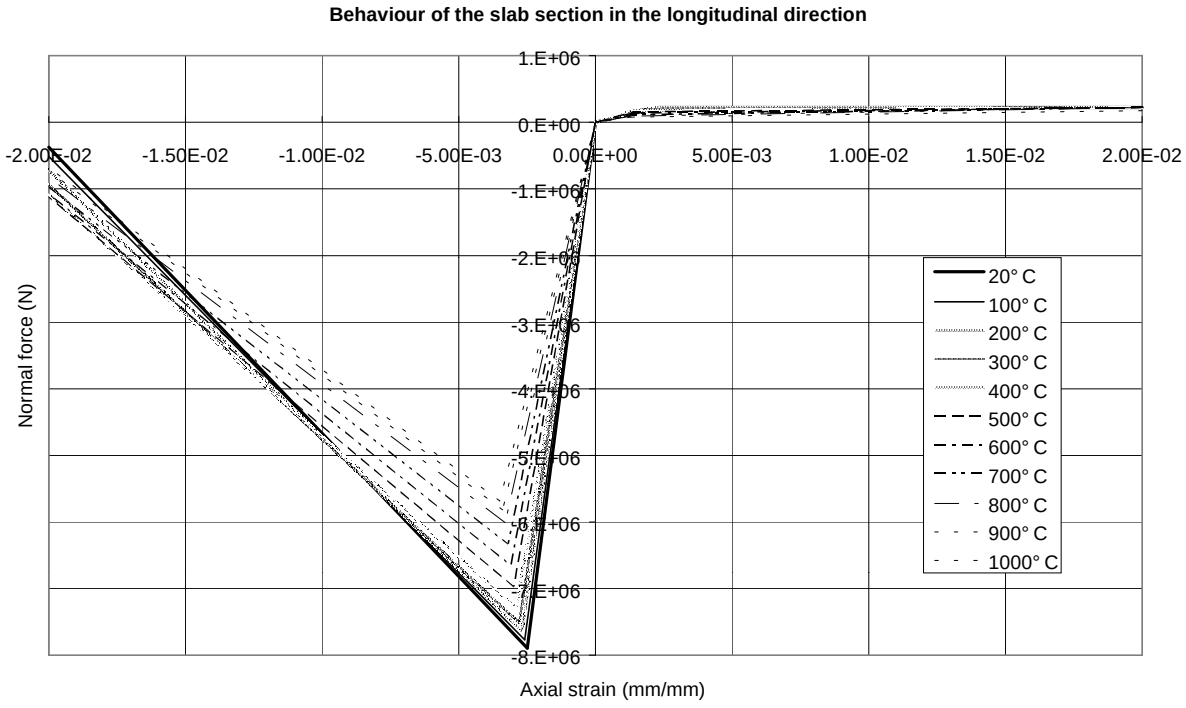

Figure 7

Axial Force- Axial Strain relationship at high temperature in the longitudinal direction

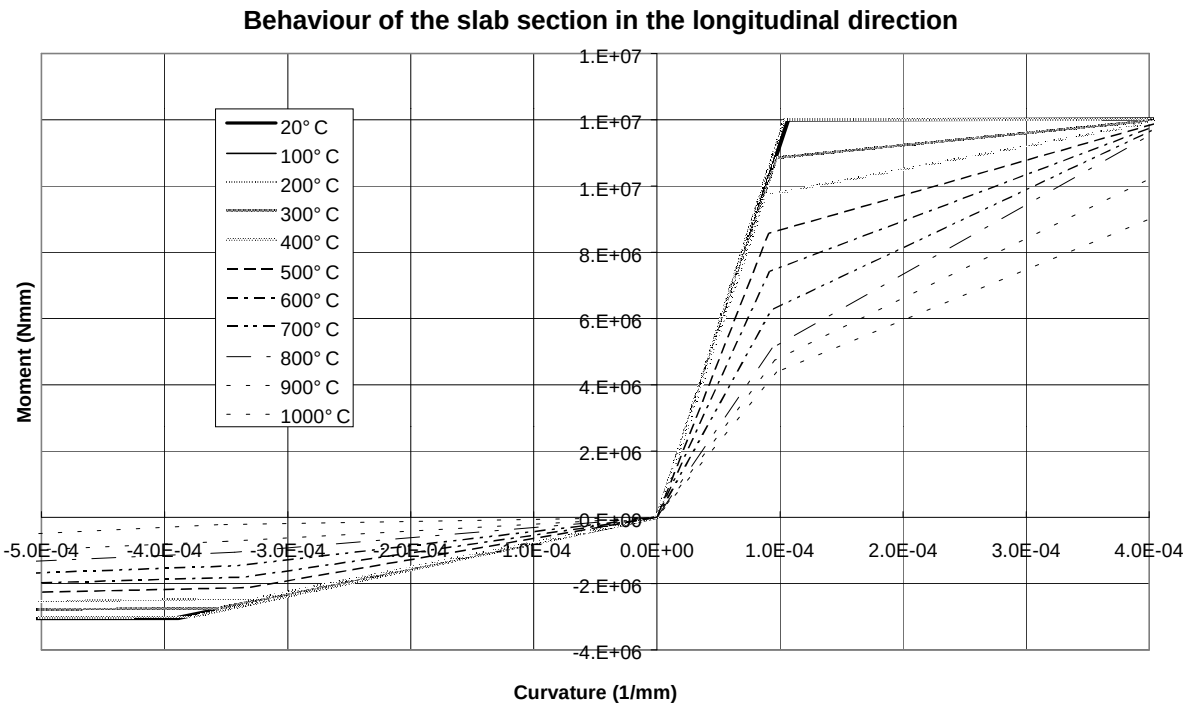

Figure 8

Moment-Curvature relationship at high temperature in the longitudinal direction

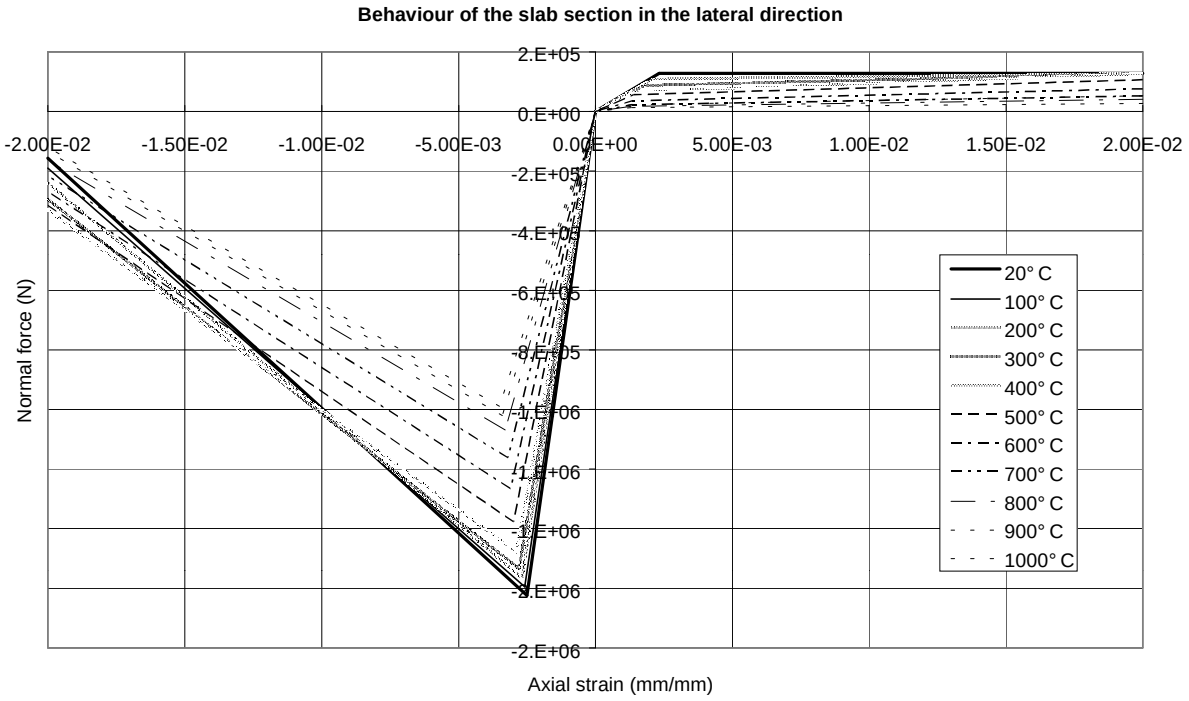

Figure 9

Axial Force- Axial Strain relationship at high temperature in the lateral direction

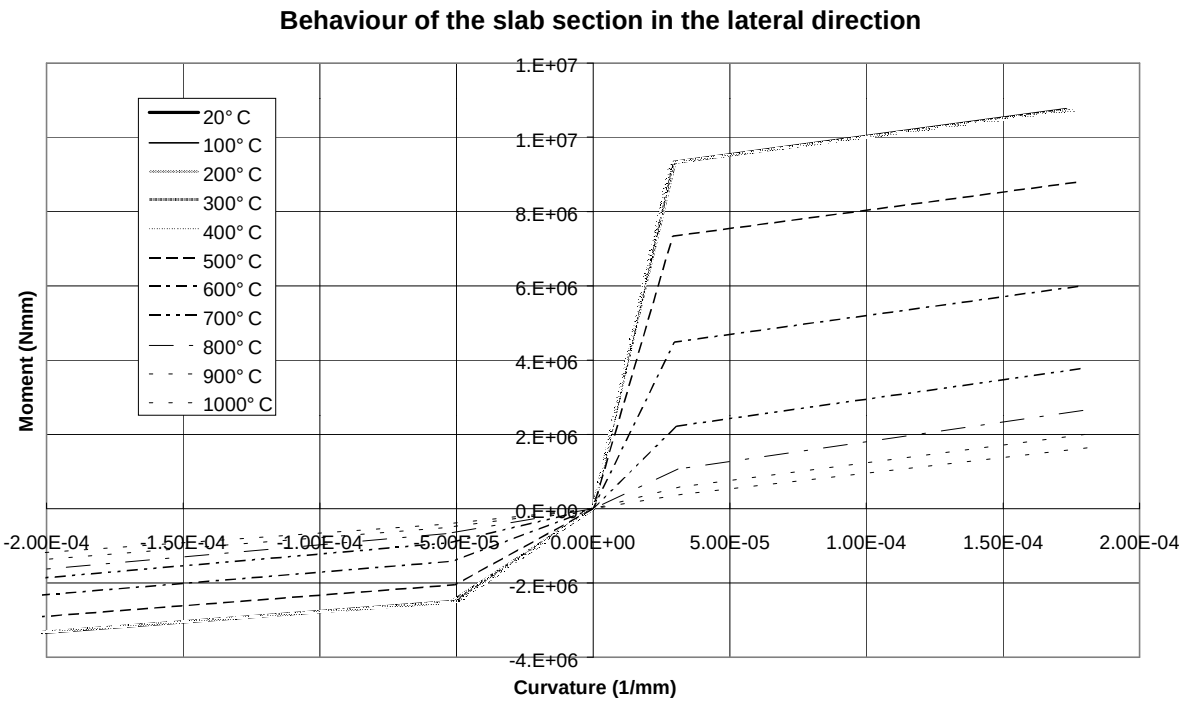

Figure 10

Moment-Curvature relationship at high temperature in the lateral direction

3. CONNECTIONS BETWEEN MEMBERS

The beam models for the longitudinal action of the slab are connected to the joist using rigid beam connection. This provides a rigid beam between two nodes to constrain the displacement and rotation of the slab's node to the displacement and rotation of the joist's node, corresponding to the presence of a rigid beam between the two nodes. The vertical separation of the joist centroid and the longitudinal slab is properly modelled. The centroid of the longitudinal slab is taken as 35mm below the slab surface and the thickness of the longitudinal slab as 70mm. The effective width of the longitudinal slab is taken as 2250mm throughout the length of the internal secondary beams and half this width for the edge beams.

For the transverse action of the slab the compatibility of deflection with the secondary joists was assured using pin connection at the crossing points to allow large deflection and large rotation in the model. The vertical separation between the secondary joists centroid and the transverse slab is properly represented, with the centroid of the transverse ribs taken as 55mm below the slab surface. All secondary beams (joists) have a composite slab connected to it.

For the steel connection, the end of the each secondary beam (joists) is connected to the primary beams (joists), in case of beam to beam connection. Each primary beam has a composite slab connected to it in a similar way as for the secondary joists. In case of beam to column connections, the secondary or primary beams are connected to the column at the level of their centre line.

4. BOUNDARY CONDITIONS

The columns are completely fixed at the bottom end and free to displace vertically at the top end. Column rotation about the vertical axe is fixed at the level of the connection with the beams. For the steel joists, the rotations about the joist axis and the vertical axis are restraint. Parallel to the primary beams, the interaction with the surrounding structure at the internal limit of the model is assumed to be symmetrical conditions where longitudinal displacements and rotations about transverse horizontal axis are fixed for the primary joist. In the other direction, the interaction with the surrounding structure at the internal limit of the model is also defined assuming symmetrical condition where the transverse displacements and rotations about the longitudinal axis are restrained for the slab end.

Each longitudinal slab is connected to a secondary beam (joist), thus have same boundary conditions as the joist below it (symmetrical conditions at mid-span). The longitudinal slab above each secondary joist is connected to the longitudinal slab over the adjacent joist in case of beam to column connection. The longitudinal slab above each secondary joist is connected to the slab over the primary beam in case of beam to beam connection. For the transverse slab: the slab is treated as translationally and rotationally continuous over the secondary beams. The rotations about vertical and lateral directions are fixed at the far end points, which are fixed against horizontal displacement in the direction of the rib axis, and horizontal displacement normal to the rib axis. These points are free to move vertically (perpendicular to the plane of the slab).

5. LOADING

5.1. Distributed load

The self-weight of the structure and the live load applied during the test are combined to give an imposed floor load of 5.48KN/m^2. In the numerical model a distributed load of 5.48 kPa is applied to the slab by means of the uniformly distributed loads on the ribs of 1.644 kN/m. This is maintained at constant value throughout the thermal loading process. Non linear geometric and material effects were modelled based on the large deformation theory using the Newton-Raphson method.

5.2. Thermal load

The effect of fire on the structure is modelled by increasing the temperature linearly over 2 steps, from ambient temperature to the maximum temperature reached for each member respectively. The thermal effect on the structure was modelled by considering both, the expansion of each element and the thermal gradient across its section. These two factors are applied to the reinforced concrete slab as well as the joists. Thermal loading is applied only to the compartment heated zone and outside it according to the test measurements. It is applied by defining the final temperature over each joist and assuming a linear variation from the initial temperature (0°C) to the final temperature. Each joist has a centroid constant temperature along its total length and has a vertical variations in temperature across its section. The vertical variations in temperature are included as a direct input following the test measurements. Temperature gradients are modelled in both the slab and the joist. For the beam finite elements adopted here, the temperatures are defined at five points across the joists section (the centroid and 2 points in each flange). The extreme fibre temperature of the lower

flange of the secondary joist on grid line 2 (**Figure 1**) is used here as the Reference temperature (RLFT). It is the average of the input temperature values for the 2 points on the lower flange.

For the slab, only the zone within the compartment is heated. The parts of the slab which lie outside the compartment zone are treated as remaining at ambient temperature at all times. The heating effect for the slab (membrane and gradient values) are applied both to the longitudinal slab and the transverse slab models separately. The temperatures of all points in the slab which lie within the compartment are treated as equal at a given height within the slab. Each rib has a constant temperature over its heated length and is considered to be at ambient temperature outside the furnace. It may be noted here that the temperature applied to the slab is the mean temperature acting on its geometric centre and the gradient across its thickness is the mean gradient deduced from the temperature distribution calculated separately for the longitudinal and the transverse directions. Figure 11 shows an example of the mean temperature measured during the fire for the slab and the beams at different location inside the fire compartment. In the model, the temperature varies from one beam to another according to the measured temperatures after 75 minutes. In this report the default temperature chosen to describe the different phenomena during the test is the temperature of the lower flange of the beam on grid line 2.

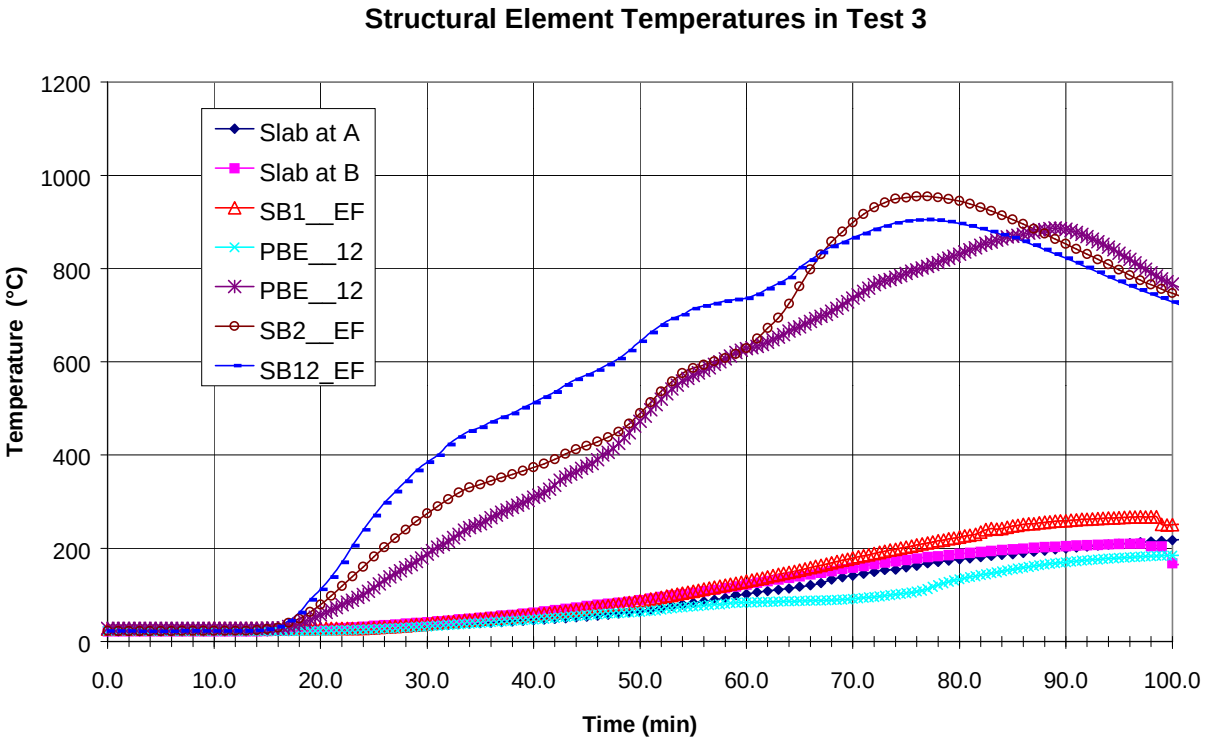

Figure 11

Temperatures in the joists and the slab inside the fire compartment

For the steel elements in the numerical model, the time lag between the lower flange temperature and the upper flange temperature is represented by assuming a linear increase in the difference between the LFT and the UFT, Table 3 shows the temperature profile applied for each of the steel members with initial temperature starting from 0 at ambient temperature.

	Step 1			Step 2		
	LFT	CT	TFT	LFT	CT	TFT
SB1__EF (protected)	120	120	96	270	270	216
SB12_EF	690	690	552	760	950	950
SB2__EF	690 (RLFT)	690	552	1000 (RLFT)	1000	800
PBE__12	600	600	480	800	800	720
PBF__12 (protected)	120	120	96	120	96	216

Table 3

Thermal loading for the steel elements

The relationship between the reference lower flange temperature (LFT = T1) and the slab centroidal temperature (SCT = T2) is characterised by a bi-linear relationship with the following co-ordinates (T1,T2): (0,0), (200,690) and (400,1000). The relationship between the lower flange temperature (LFT = T1) and the slab temperature gradient (SGT = DT3) is characterised by a bi-linear relationship with the following co-ordinates (T1,DT3): (0,0), (1000,3) (i.e. the centroidal temperature and the gradient are arranged to give the top surface of the transversal slab rising to 205 degrees at the end of the test, whilst the lower surface reaches 595°C when the reference lower flange temperature reaches 1000°). Table 4 gives the temperature evolution during the 2 simulation steps for the slab in the longitudinal and transverse directions. To be noted here that the slab temperature was higher then in the test (400°C instead of 300°C). In fact the mean uncertainty over the right values for the temperature acting over the slab thickness led to assume a higher value in the numerical model to achieve the correct deformed shape.

	Step 1		Step 2	
	Centroid	Gradient	Centroid	Gradient
Slab in transverse direction	200	3	400	3
Composite slab (Primary beams)	195	2	390	2
Composite slab (Secondary beams)	200	3	400	3
Edge composite slab	100	2	260	2

Table 4

Thermal loading for the slab elements

6. COMPARISON WITH TEST DATA

6.1. Deflection of primary beams

Many measurements were taken over all the heated joists. The maximum deflection observed for each joist was at mid-span. Here we compare the numerical prediction of the maximum deflection with the experimental results. First comparison is for the heated primary beam on grid line-E. The first measurement point is located on the bottom flange of the beam at mid-span. Figure 12 shows the relation between the deflection of the beam at this point and the reference temperature of the lower flange of the hottest joist (SB2__EF) at mid-span. The negative sign for the deflection indicates a vertical displacement downward. In both the finite element analysis and the experiment, the deflection increases with temperature and the experimental measurements show a non-linear relationship with three major patterns. First a from 0 to 600°C (RLFT) with a non linear increase of deflection against temperature, then from 600°C to the 900°C with an overall linear pattern characterised by a flatter slope, then a final stage from 900°C to 1000°C where the deflection increase rapidly against the temperature. In this last phase the rapid increase in deflection is due to a rapid increase in the slab temperature, which combined with the steel joists temperature produces the overall thermal regime applied to the composite slab.

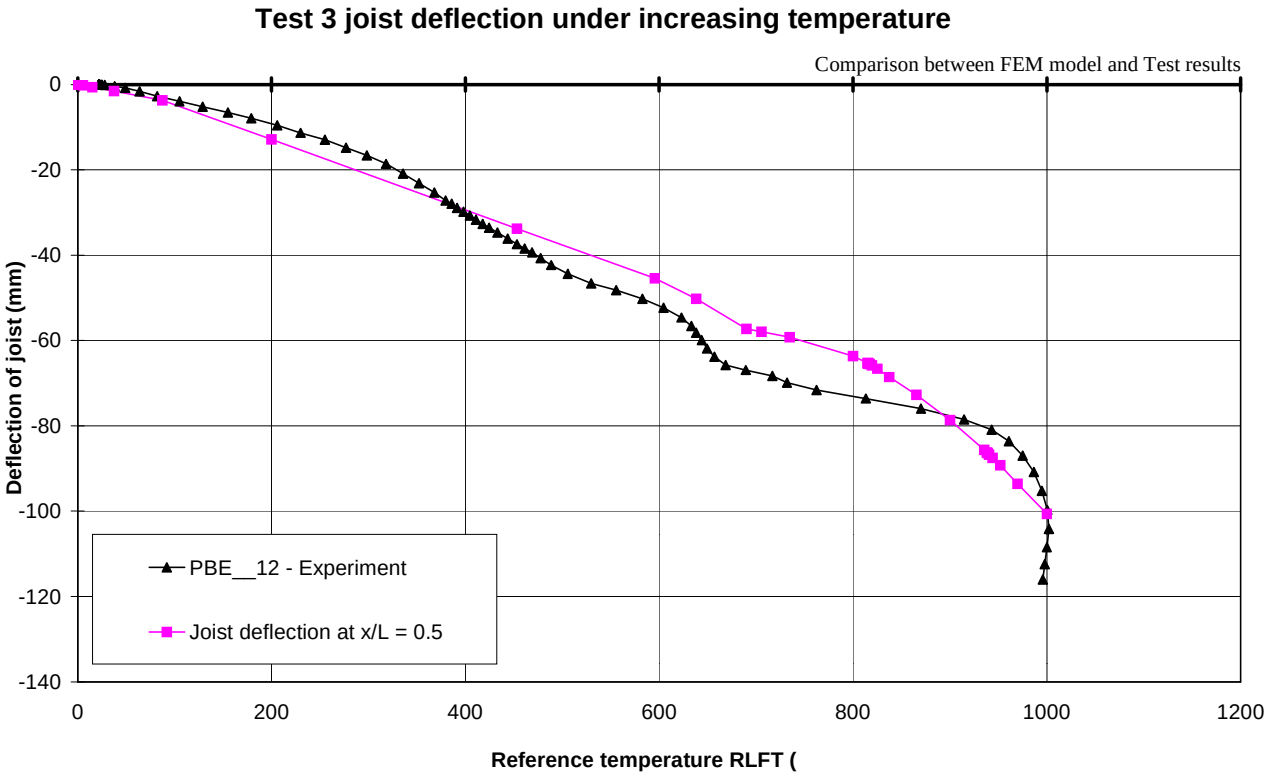

Figure 12

Deflection of the heated primary beam at mid span

In the finite element analysis we can distinguish two main patterns, first from 0 to 690°C where the deflection increasing with nearly a linear relationship, followed by the second phase up to 1000°C in

which the relation becomes non-linear with a rapid increase of the deflections against the time. The deflection predicted by the numerical model reaches the same final value of 100mm at 1000°C, with close values all the way during the fire. The maximum difference between the model and the test is approximately 10mm and recorded near 700°C. The difference between the model and the test can be attributed to the approximated temperatures applied over mainly the slab. To be noted here that the measurement of temperature over the slab was insufficient to give a complete spatial distribution (only 4 location over the 80m^2 of heated zone).

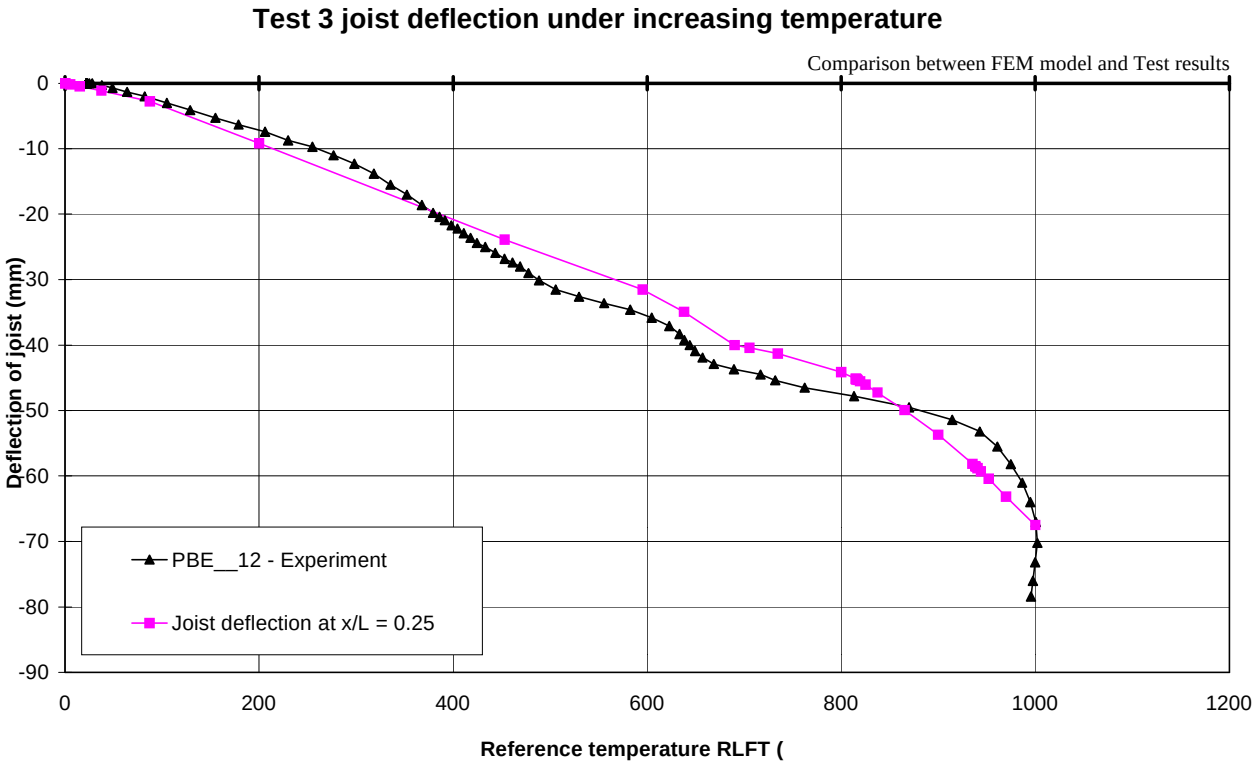

Figure 13

Deflection of the heated primary beam at Y/H=25%

To ensure that deflected shape of the beam is coherent between the model and the experiment, the deflection at a second point along the primary beam is compared on Figure 13. The point is located on the lower flange of the beam at 1.5m from the column (**Figure 1**). We can observe the same patterns as at mid-span in both the experiment and the numerical model and the values predicted are close to the measurement, indicating that over the primary beam the model is predicting the correct deflections. To be noted that the shape of the deflection-temperature curve is governed by the deflection of the beam related to the reference temperature chosen, the last steep increase in the test measurements between 900°C and 1000°C is really due to the relative rate of heating of the whole structure (slab and joists) against the reference joist rate of heating only. At this final stage the reference joist had a very low temperature rate of heating which reached 1000°C then started to decrease again, while in the numerical model the calculation ends at the maximum temperature, this explains the difference of shape between the two curves (test against model).

6.2. Deflection of secondary beams

Here we compare the numerical prediction of the maximum deflection with the experimental result. First comparison is for different secondary beams. The first point of comparison here is located on the secondary joist on grid line 2. This joist was connected to a column at each end and the maximum deflection was obtained at mid-span. On Figure 14 we can see that the behaviour is mainly be divided into two part, from 0 to 690°C the relationship is approximately linear, from 690°C to 1000°C a steep increase of deflection against the joist temperature, the first part of the relationship is very similar to the pattern observed in Test1 for a similar restrained secondary beam (Sanad)[11].

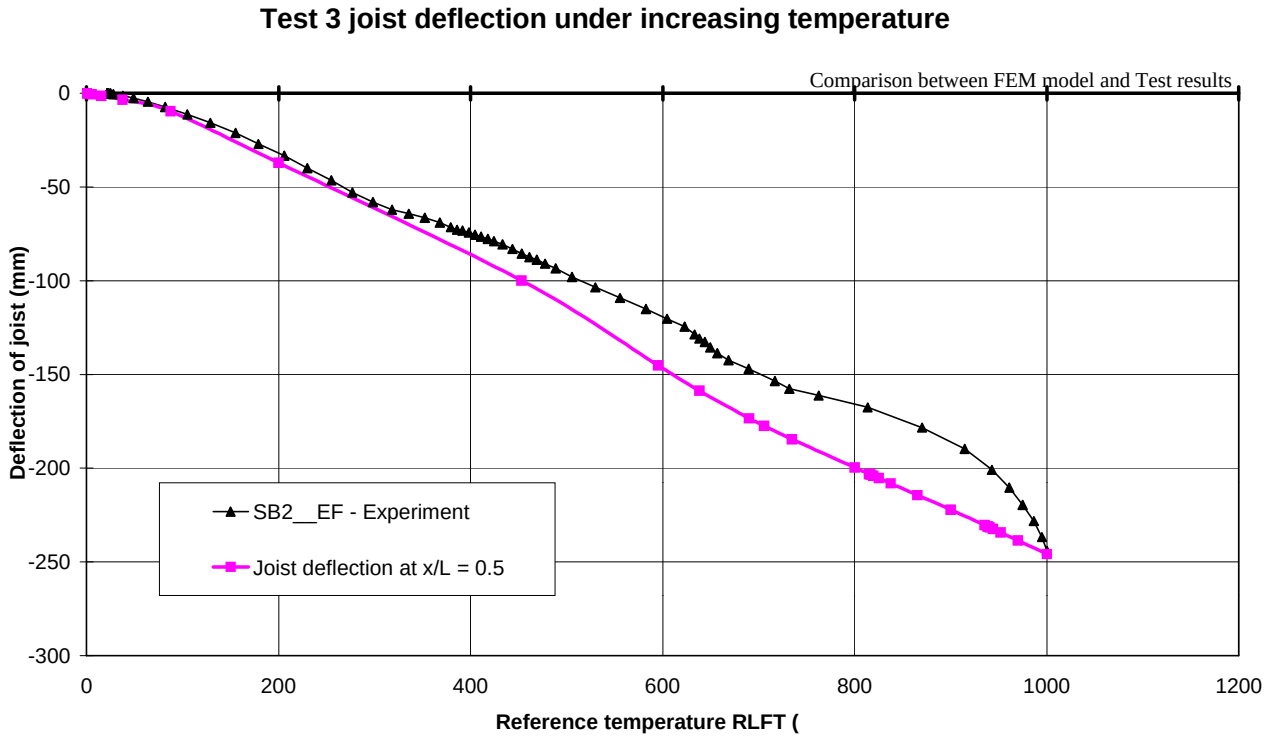

Figure 14

Mid span deflection of the heated secondary beam on grid line 2

The second part of the behaviour is identical the last pattern observed for the primary beam and is mainly due to the temperature regime applied to the structure at the end of the fire. The numerical predication are in good agreement with the measurement for most of the fire time and the difference observed in the 2 curves at the end of fire is again related to the temperature regime applied to the structure.

Over the whole structure the most deflected beam is the one between the grid line 1 and grid line 2. This secondary beams is connected at both end to primary beams, thus the total deflection for this beam includes the deflections of the primary beam supporting it. Figure 15 shows the deflection curve at mid-span of the joist. Again we can observe the two patterns for the deflection-temperature relationship. The difference between the model and the experiment in this case is more pronounced with a maximum deflection of 320mm obtained from the calculation against 370mm from the

measurements. Here again the uncertainty of the slab temperature during the test, specially in the transverse direction, is important as the ribs temperature play a very important role in the development of alternative load carrying mechanism in the transverse direction (by tensile membrane action). According to the temperature reached in the transverse direction, the ribs can alter or prevent the composite beam from further deflection specially at the end of the fire where the joist axial capacity is very low due to the large properties degradation of the steel at the latter stage of fire.

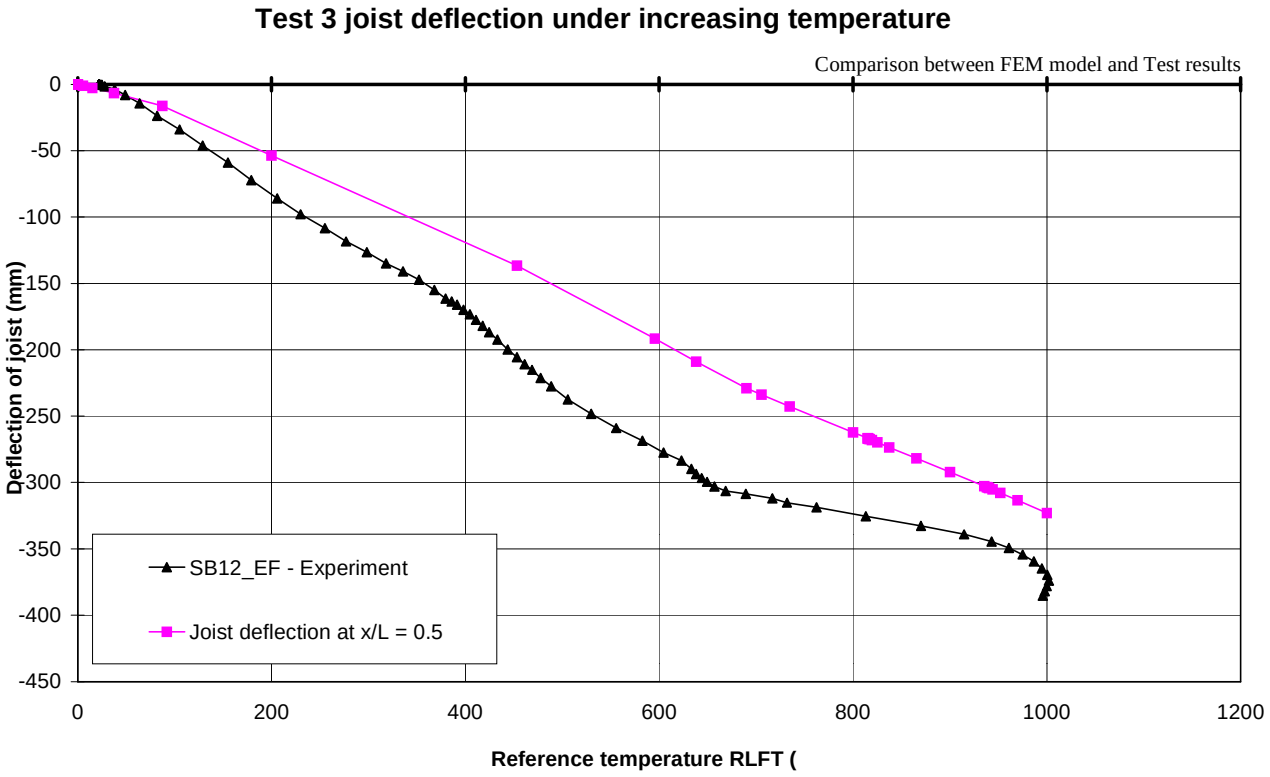

Figure 15

Mid span deflection of the heated secondary beam between grid 1 and 2

6.3. Deflection of edge protected beams

Two further comparisons of deflections are carried out for the edge protected beam. The first edge beam is parallel to the secondary joist and connected to columns at both ends. The comparison is shown on Figure 16, we can notice that the trends are generally comparable in both the numerical model and the experiment. The maximum deflection obtained is of the order of 10mm which is relatively low, this because the successful measurements over this joist were obtained near the columns ends.

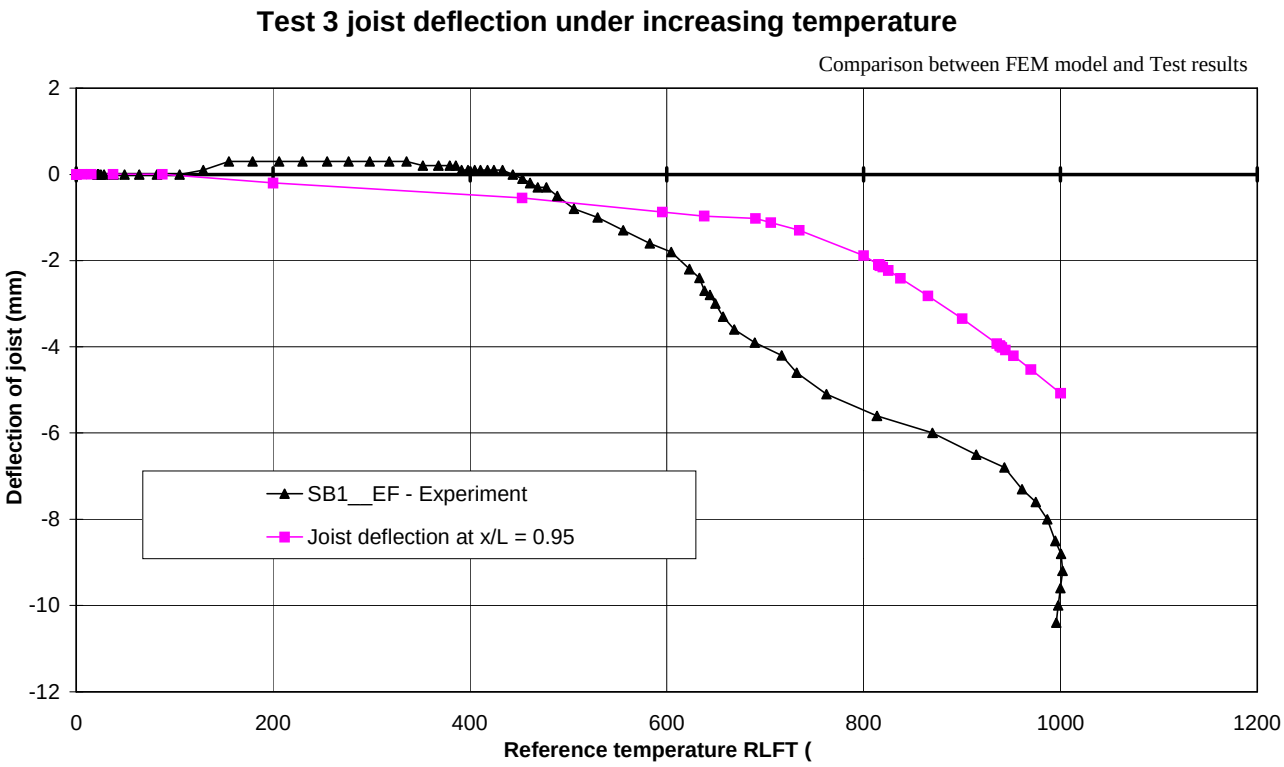

Figure 16

Mid span deflection of edge protected secondary beam on grid 1

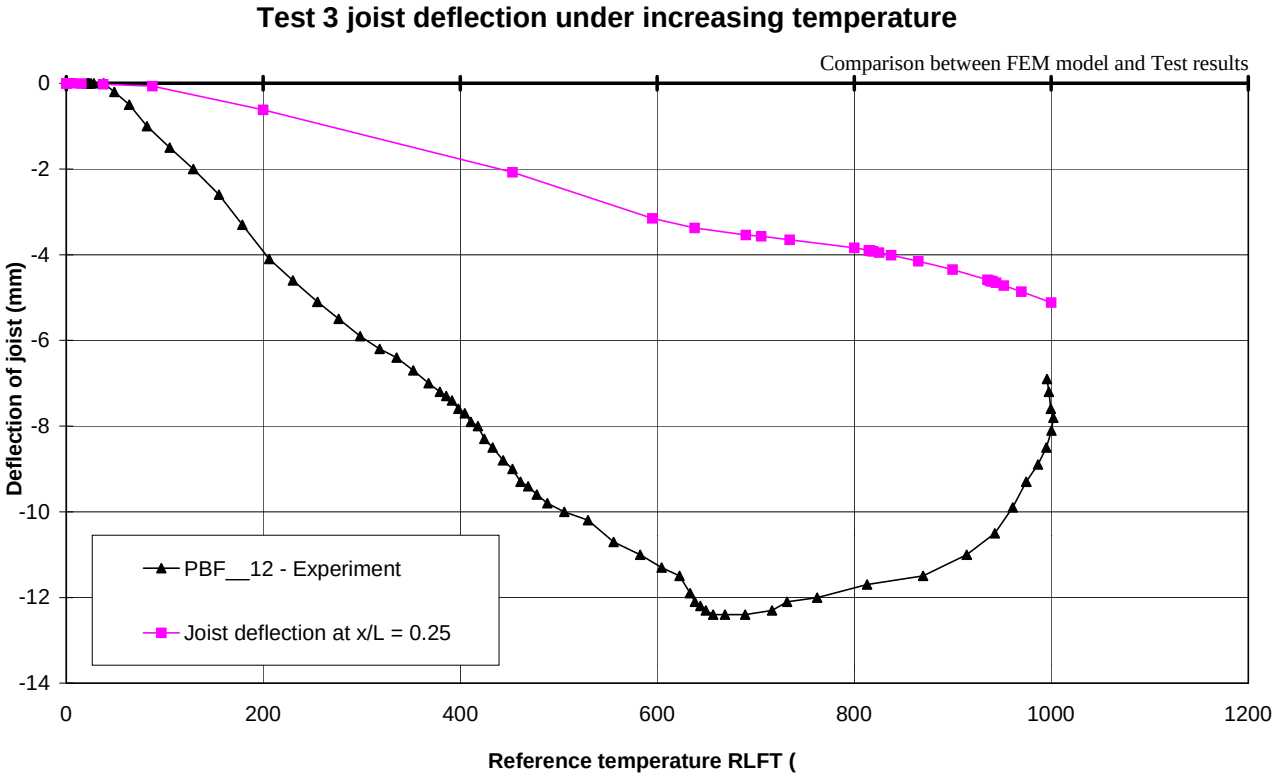

Figure 17

Mid span deflection of edge protected primary beam on grid F

The final comparison is carried at 25% of the span of the edge beam parallel to the primary beams. Here we can notice that the trend is different in the model and the experiments. In the model the deflection is nearly linear from the start to the end (Figure 17). In the experiment the deflection increases from 0 to 640´C then reduces up to the end of the fire. The reason of such behaviour can be related to the fact that the edge composite beam has a relatively low torsional stiffness, thus during the last stage of the fire (640°C onward) this beam rotate and displace horizontally instead of vertically. Hence it has an increase of curvature in the horizontal plan which can easily dissipate the extra length obtained from the thermal expansion. To be notice that the final temperature measured over the primary protected edge beam was of the order of 250°C. This explains as well the low deflection values obtained over this beam (12mm at end of heating).

6.4. Horizontal displacement of columns

A comparison was made for the horizontal displacement of the columns above the floor, where transducers were installed to measure the horizontal displacements of columns. For the column E1 connected to the heated primary beam, the measured displacement are compared with the numerical predictions in Figure 18. The horizontal displacement is plotted against the reference temperature of the joist lower flange at mid-span the positive sign indicates a horizontal displacement towards the outside of the building on the axis of the primary beam.

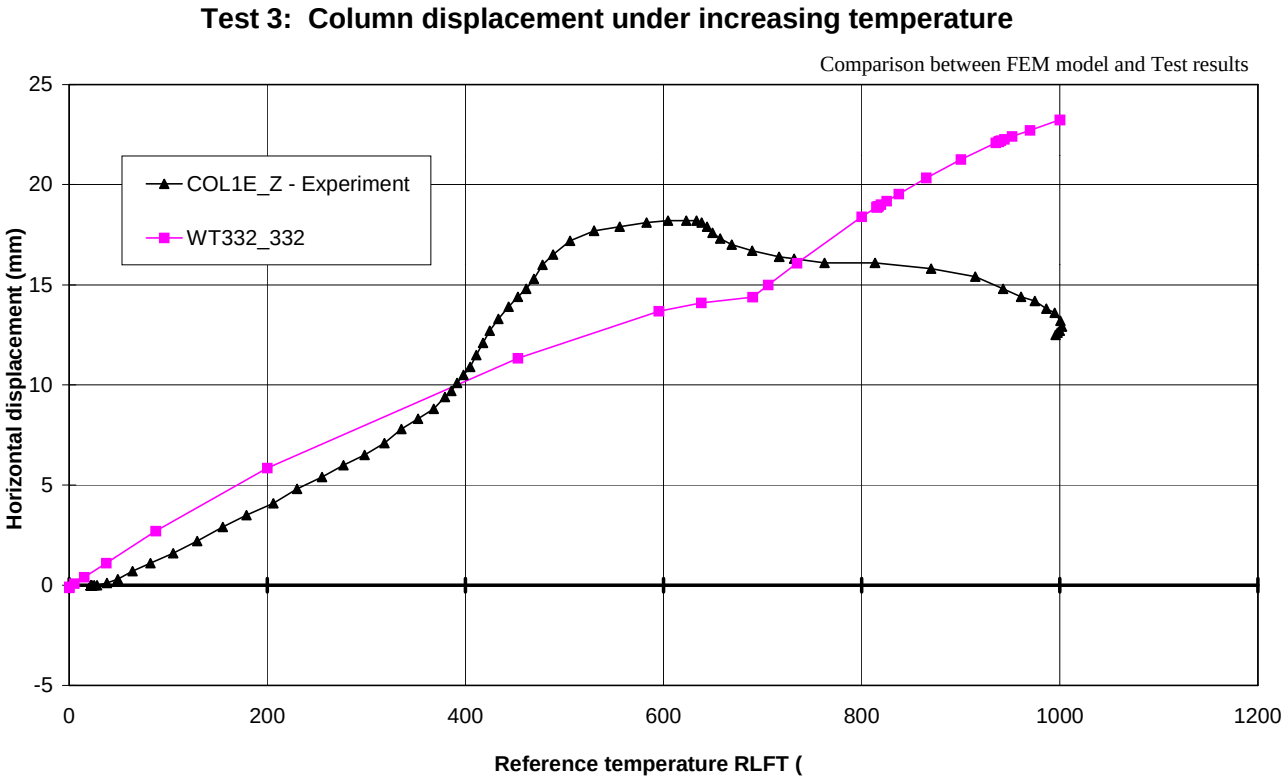

Figure 18

Horizontal displacement of column E1 in Y direction

The comparison here shows that order of magnitude of the displacement obtained from the numerical model is comparable with the test results. The model predicts 23mm of column displacement outside the building against nearly 15mm for the test. In the test the horizontal displacement reaches a maximum value between 500°C and 600°C then it displaces in the opposite direction (toward the inside of the building) till the end of the heating regime. In the numerical model the displacement is steady toward the outside of the building from the start to the end of the fire with a variation at 690°C corresponding to the change from step1 to step2 in the modelled heating temperature and the difference between the shape of the curves in the experiment and the numerical model can be related to the simplified heating regime adopted in the model.

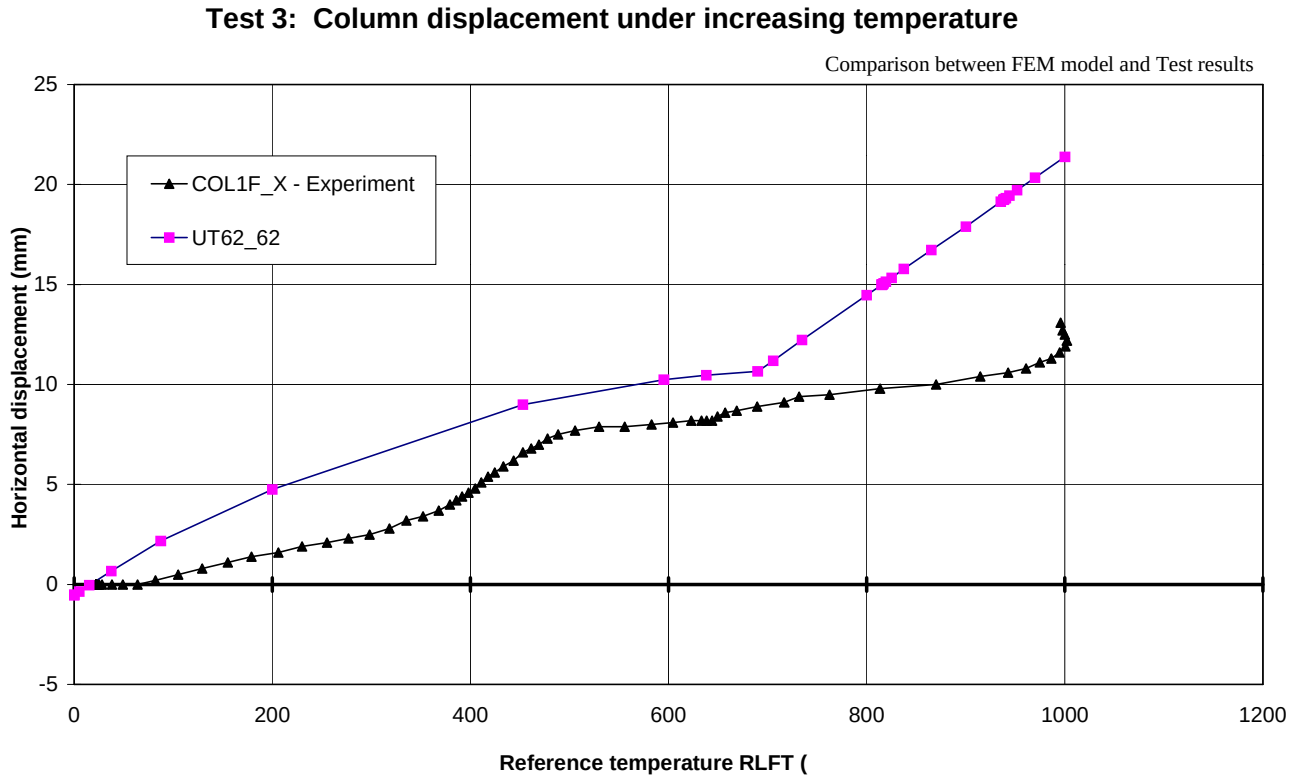

Figure 19

Horizontal displacement of column F1 in Y direction

The following comparison is carried for the horizontal displacement of the corner column (1F) in the direction of the secondary beam (X). The shape of the curves in the model and the test are near to each other. The model predicts an increase in the horizontal displacement from 0 to 400°C then a plateau to 690°C followed by a linear increase to the end of the test. The magnitude of the horizontal displacement is 12mm at end of fire in test against 22 in the model. The direction of the displacement is directed again outside the building on the axis of the edge protected secondary beam indicating that the floor is expanding the x direction and the y direction as obtained from the previous comparison. This important aspect of the behaviour of the slab is predicted in the numerical model and agrees with the test measurements.

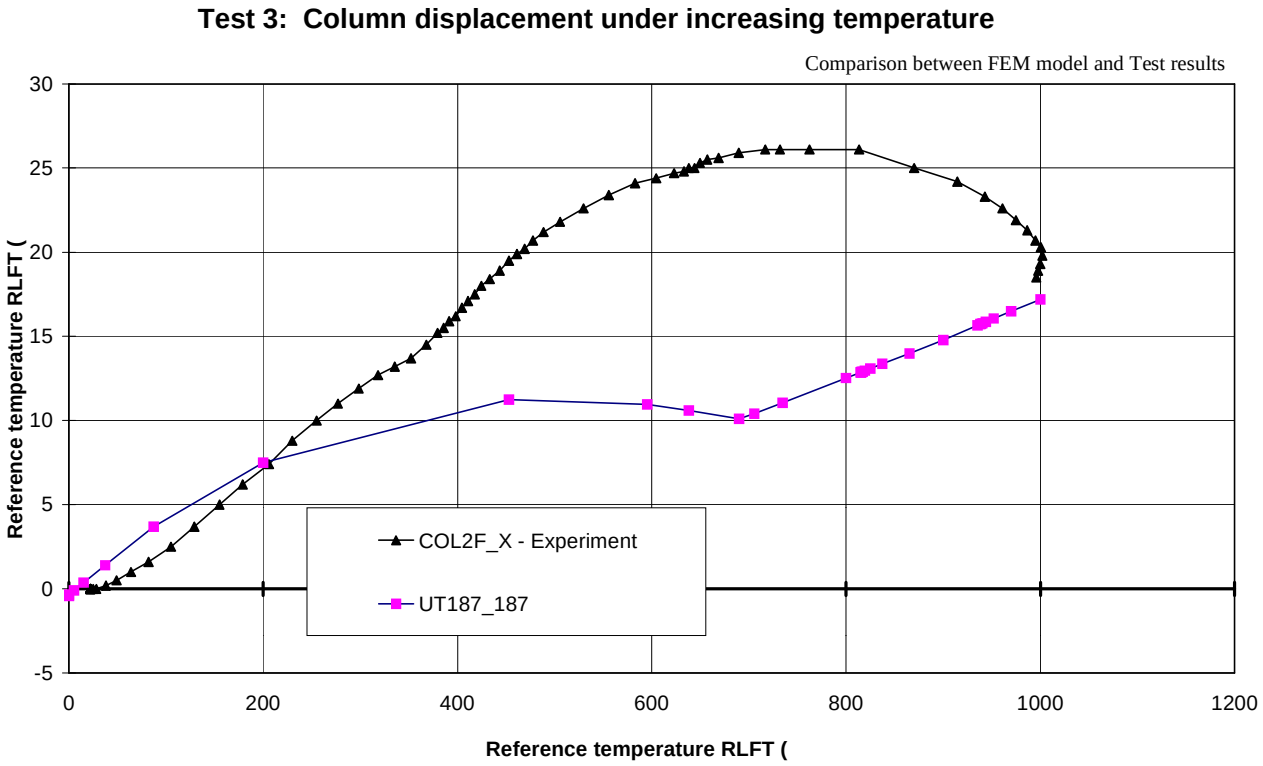

Figure 20

Horizontal displacement of column F2 in X direction

The last comparison is carried for the external column (2F) connected the secondary beam SB2__EF. Again the model shows a positive displacement of the column due to the expansion of this heated beam. The test again shows an initial linear increase in the horizontal displacement which reaches a plateau at 650°C then the columns start moving to the inside of the building till the end of the fire while the model predicts again an initial non-linear increase followed by linear increase from 690°C to the end of the heating regime.

From the above comparisons, between the finite element predictions and the test measurements, we can see that the numerical model is in agreement with the test, for different quantities and over the total time of the fire and the different approaches used in the model, described above, can predict with acceptable accuracy the global behaviour of the structure under fire conditions.

7. CONCLUSION

In this paper we described a finite element model developed to simulate the third full-scale fire test carried by British Steel in the large building test facility at Cardington. The test was dedicated to study the behaviour of the structure under a corner fire. The composite action between the slab and the beam was modelled in the model by means of rigid elements coinciding with the shear stud locations. The connections between different steel members were modelled by imposing displacement constraints to the nodes of the members. Using the general purpose finite element

program ABAQUS, a numerical model capable of predicting the behaviour of the composite framed structures under fire condition was developed.

The results of the numerical model were compared with the experimental measurements at six different locations in the compartment, inside the heated zone and at the edge protected beams. The comparisons showed good agreement between the model and the test measurement for the total time of fire at different points of the unprotected beams. The horizontal displacement were also compared for three different columns and showed an agreement on the general trend of the floor expansion toward the outside of the building. The finite element model developed in this paper has been developed with the aim of understanding local and global structural behaviour during fire and the more details on the structural behaviour during this test is to be published in the near future.

8. REFERENCES

1. Abaqus (1994) : Abaqus theory manual and users manual, version 5.4, Hibbit, Karlsson and Sorensen Inc., Pawtucket, Rhode Island, USA

2. P.N.R. Bravery (1993): Cardington large building test facility, Construction details for the first building, internal report British Steel plc.

3. D.J. O'Connor and al. (1995) : Determination of the fire endurance of model concrete slabs using a plastic analysis methodology, The Structural Engineer, Volume 73, No 19/3.

4. Eurocode 2 (1995) : Design of concrete structures - Part1-2 : General rules - Structural fire design, ENV 1992-1-2.

5. Eurocode 3 (1995) : Design of steel structures - Part1-2 : Fire resistance, ENV1993-1-2.

6. Eurocode 4 (1994) : Design of composite steel and concrete structures - Part1-1 : General rules and rules for buildings, ENV 1994-1-1.

7. B.R. Kirby (1995) : Behaviour of a multi-storey steel framed building subject to natural fires: Test3-restrained beam, deflection measurements, Document ref; S423/1/Part D1, British Steel plc.

8. B.R. Kirby (1995) : Behaviour of a multi-storey steel framed building subject to natural fires: Test3-restrained beam, temperature measurements, Document ref; S423/1/Part T1, British Steel plc.

9. Rotter, J.M., Sanad, A.M., Usmani, A.S. and Gillie, M. (1999) "Structural performance of redundant structures under local fires", Proc., Interflam '99, 8th International Fire Science and Engineering Conference, Edinburgh, 29 June - 1 July, Vol. 2, pp 1069 - 1080.

10. Sanad A.M. "British Steel Fire Test1: Reference ABAQUS model using grillage representation for slab" Research report R99-MD1, University of Edinburgh, Department of Civil and Environmental Engineering (December 1999).

11. Sanad A.M. “British Steel Fire Test3: Reference ABAQUS model using grillage representation for slab” Research report R00-MD10, University of Edinburgh, Department of Civil and Environmental Engineering (February 2000).

12. Sanad, A.M., Rotter, J.M., Usmani, A.S. and O'Connor, M.A. (1999) "Finite element modelling of fire tests on the Cardington composite building", Proc., Interflam ’99, 8th International Fire Science and Engineering Conference, Edinburgh, 29 June - 1 July, Vol. 2, pp 1045 - 1056.

13. Sanad, A.M., Lamont, S., Usmani, A.S. And Rotter, J.M. (2000)[1] " structural behaviour in fire compartment under different heating regimes – part 2 (Slab mean temperatures)" Fire Safety Journal, accepted for publication May 2000.

14. Sanad A.M., Rotter J.M., Usmani A.S. and O’Connor M.A. (2000)[2], “Composite beam in buildings under fire – numerical modelling and structural behaviour”, Fire Safety Journal, accepted for publication June 2000.